Influence of axially structured catalyst in reverse flow reactor on the hybrid N_2O decomposition

K. Nalpantidis, F. Platte*, D.W. Agar, S. Turek

September 15, 2004

Abstract

The fixed-bed reactor with periodical flow reversal allows a stable autothermal operating condition, even for a weak exothermal reaction. Periodical flow reversal has also been proposed for the combustion of gases with traces of N_2O. It is a fact that higher temperatures can lead to a hybrid reaction, i.e. in addition to the heterogeneous-catalytic reaction a homogeneous-thermal combustion takes place. The following investigates the influence of axially structured monolith catalyst on the hybrid N_2O decomposition in order to understand the coupling mechanisms in more detail. Recent studies prove the potential of the direct calculation of cyclic-steady states which transform the usual initial-value problem into a steady-state boundary-value problem. In combining this technique with standard bifurcation analysis tools, it is now possible to study the influence of key parameters on the process in a very efficient and elegant way. Both, simulations and experimental investigations were required to design an appropriate setup for a spatial and temporal separation of the two underlying types of reaction.

Keywords: Combustion, Hybrid reaction, Fixed bed reactor, Autothermal operation, Periodic flow reversal

1 Introduction

Over the last decades the field of chemical engineering has witnessed an increased interest in unsteady-state processes. One such process is the reverse-flow-reactor (RFR) which is operated in a forced periodical way by switching the side/direction of the inflow [26]. One of the most notable advantages of the reverse-flow concept is certainly that due to the regenerative heat recovery a hot reaction zone, surrounded by two cold zones is trapped in the centre of the fixed-bed. Due to inherently low loss of heat, even weak exothermic processes (or alternatively processes with trace gases) can remain ignited without additional external heat or fuel gas. Suggested examples for industrial application are the catalytic treatment of waste gases in air and oxidation of SO_2 [27] and many more [28].

The characteristical behaviour of two parallel exothermic reactions (propane/ propene) in reverse-flow operation have been investigated experimentally by Nieken and Eigenberger [31] and theoretically by Salinger and Eigenberger [19] [20]. They found an interesting setup of multi-steady-states (MSS). To a certain extent, a hybrid reaction can be regarded as kind of a parallel reaction and that is why MSS can also be expected in the case of hybrid reactions.

*Corresponding author. *E-mail address:* fplatte@math.uni-dortmund.de (F.Platte)

More recent work from Glöckler, Kolios and Eigenberger [10] is closely related to the idea of a structured catalyst. However, it considers only one non-hybrid reaction (either exothermal and endothermal) in each halfcycle and is therefore chemically speaking a totally different kettle of fish.

Working in the vicinity of high temperature catalysis can lead to a hybrid reaction, i.e. in addition to the heterogeneous-catalytic reaction a homogeneous-thermal combustion can take place. Hybrid reactions may be unwanted as they can irreversibly harm the activity of the catalyst or damage the monolith structure. From the reaction engineering point of view, others claim that hybrid reactions could have advantages in the process regarding reactor performance, yield and selectivity [30] – if designed in the right way. In any case, hybrid reactions are still poorly understood. Moreover, working on elevated temperature levels due to thermal radiation, the assumption of an adiabatic condition in the reactor does not hold any more. As a result, for simulation purposes heat losses must be considered. The influences of heat losses in RFR has extensively been investigated by Khinast and Luss [8], who considered sinks and sources in the energy equation.

There are many design as well as operating parameters, such as reactor length, flow rate, inlet concentration, switching time and physical and chemical properties of the catalyst, whose influence on the entire process might be very complex. Numerous scientists have been working on the mathematical description of the RFR in order to improve the understanding of the whole process behaviour. Most of these models are comprised of one-dimensional, time-depending balances of convection-diffusion-reaction type.

Bifurcation analysis techniques can easily be applied if founded on the stationary formulation of the direct calculation – regardless of being based on a global discretization or shooting method. With the aid of these techniques, extinction-ignition diagrams and other parameter studies can be calculated in a very efficient way. In particular, the complete solution branch comprised of stable and unstable steady states can be obtained. This cannot be derived from a simple dynamical simulation approach.

In this paper we present our experimental and computational investigation of the hybrid (catalytic/thermal) decomposition of dinitrogenoxid (N_2O) in a RFR on a technical scale. In contrast to parallel reactions, such as the propane/propene reaction, it is not possible to control or influence the reaction pathway directly by choosing a desired inflow ratio of the two components. We therefore suggest an axially structured catalyst bed for achieving a spatial and temporal separation of the two underlying types of reaction. We will proove in this paper that an appropriate structure in combination with varying switching times can lead to the separation of the underlying elementary reactions. This behaviour is of interest especially when designing a new process which could exhibit possible hybrid reactions.

The point that we want to focus on in this paper is that the extended amount of data of such an unsteady state process may be exploited from the kinetical point of view, as one is able to understand when and where the subreactions ignite or extinguish. Axially structured catalysts in under periodical flow reversal operation can act as an improved diagnostic for qualitative model discrimination.

2 RFR model and direct calculation

Priciple of an RFR

The way in which a RFR is operated is illustrated in Fig. 1. By simultaneously opening the pair of valves V1/V3 whilst closing the pair V2/V4 or vice versa, the flow direction and inflow side is reversed. The main advantage of the periodical flow reversal concept is that a hot reaction zone surrounded by two cold zones, is trapped in the centre of the reactor bed. Matros was the first who suggested this operating condition in the thirties of the last century so that the reactor is also known as Matros-reactor. The volumetric heat capacity of the solid fixed bed, most commoly made of ceramics, is approximately a thousand times larger than the heat capacity of the gas. As a result, two phenomena can be observed. First of all, the gas flow pushes a temperature front through the reactor at a velocity which is reduced by the same factor of heat capacities. Secondly, the above mentioned difference in heat capacity results in a very slow transient behaviour – until the cyclic steady state is reached.

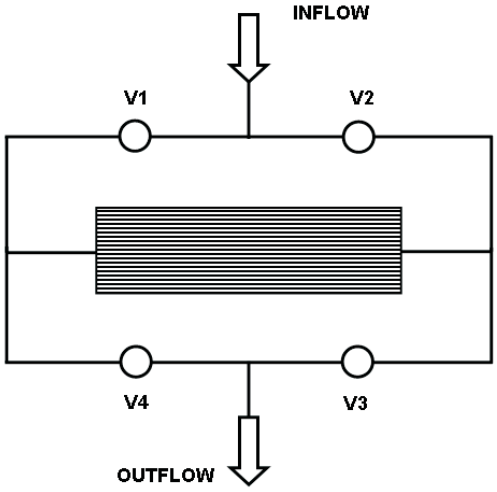

Figure 1: Schematic diagram of a reverse flow reactor. Either the pair of valves V1/V3 or V2/V4 are open at the same time.

Heat and mass balance

We chose a simple two-equation model to describe the distribution of temperature and concentration inside the reactor. The model comprises two balance equations, one pseudo-homogeneous energy balance and the other a mass balance. Both are usually partial differential equations (PDEs) in time and (one-dimensional) in space. Due to the dominating behaviour of the heat balance, we regard the mass balance as to be pseudo-steady-state. Nevertheless, since the gas phase is coupled to the reaction term, it implicitly depends also on time. The resulting system can be represented by the following expressions:

$$\begin{aligned}(1-\varepsilon)(\varrho\, c_P)_s \frac{\partial T}{\partial t} &= \lambda_{eff}\frac{\partial^2 T}{\partial z^2} - (\varrho\, c_P)_g v \frac{\partial T}{\partial z} \\ &\quad + \frac{k}{r}(T - T^{amb}) + (-\Delta H_r) r_{hyb}(T, C),\end{aligned} \tag{1}$$

$$0 = D_{eff}\frac{\partial^2 C}{\partial z^2} - v\frac{\partial C}{\partial z} - r_{hyb}(T, C). \tag{2}$$

Reaction kinetics
The TC-model (thermal coupling) considers the two reaction pathways as being chemically independent of one another – due to the heat of reaction however, the reactions depend at least thermally on one another – thus the overall hybride reaction rate r_{hyb} is simply the sum of the two contributions

$$\text{homogeneous:} \qquad N_2O \rightarrow N_2 + 1/2\, O_2,$$

$$\text{heterogeneous:} \qquad N_2O \rightarrow N_2 + 1/2\, O_2,$$

which results in the following reaction term:

$$r_{hyb}^{TC}(T, C) = \left[\frac{a_v \cdot \beta \cdot k_{het}(T)}{a_v \cdot \beta + k_{het}(T)} + k_{hom}(T)\right] \cdot C \tag{3}$$

Alternatively, the TCC-(thermal-chemical coupling) model can be selected. This model consists of a simple two-step mechanism for both individual reactions, namely the homogeneous and heterogeneous reaction pathways. The re-combination of oxygen represents the sole chemical coupling mechanism considered in this model. It should be stressed that there is no definitive verification for this model. Further information can be found in [6]. The reaction rate according to the TCC-model can be reduced to that of the TC-model augmented by a single correction term. In the present work we use the TC-model suggested as being most appropriate by previous work.

Space-time finite-difference discretization
The PDEs presented above are commonly discretized in space and then integrated in time until a cyclic-steady state is reached. Regardless of the spatial discretization technique that is used, this is referred to the method of lines (MOL). Unfortunately, this dynamical approach suffers from very slow convergence to the cyclic-steady because of the stiffness of the system. Sometimes, up to several hundred cycles must be simulated [29]. The difference of the computational domain for a dynamical and direct calculation is illustrated in Fig. 2. There it also can be seen where in time and space boundary conditions have to be set.

We applied a direct calculation method, based on global discretization, to solve the governing equations. Alternatively, a direct calculation of cyclic-steady-states can be based on a dynamical simulation wrapped by a shooting method algorithm. Both methods exhibit characteristic advantages. We chose the global discretization approach since we believe that it allows for better implementation of modern mathematical algorithms - gridding, discretization and solvers - developed for 2D/3D problems, whereby the shooting method is essentially restricted to method of lines.

Earlier research clearly shows that either approach is far more efficient than a simple dynamical simulation – if only cyclic steady states are of major interest [19] [20]. In particular, this can be said for the case of parameter studies in which hundreds of cyclic steady states must be calculated. We had to carry out such parameter studies for the desired ignition-extinction bifurcation diagrams. To save disc storage and computation time, the global dicretization has been applied only for a half-period and not for the full period. To have a well posed problem, in addition to the usual Danckwerts boundary conditions in space, we have required mirror symmetric profiles for the temperature in time (cf. (2))

$$\textbf{Mirror symmetry:} \qquad T(z, t) = T(L - z, t + \Delta t_{cyc}). \tag{4}$$

It should be noted that the (mirror) symmetry condition utilized in the direct calculation is precisely the commonly used stopping criteria in the dynamical simulation. The global discretization of the energy balance is the crucial step. We chose a two-dimensional, equidistant spaced grid to discretize over the reactor length $0 \leq z \leq L$ and switching time $0 \leq t \leq \Delta t_{cyc}$.

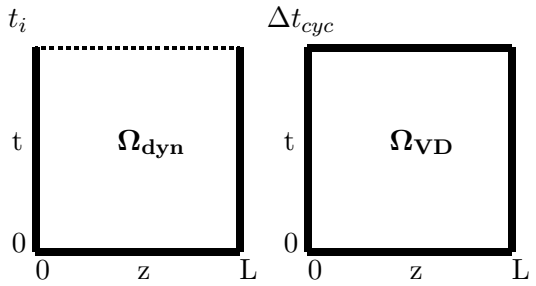

Figure 2: Computational domain of a dynamical simulation (left) and direct calculation (right). On bold lines boundary conditions must be defined

Contrary to the FEM approach suggested by Salinger and Eigenberger [19] we applied a modified Finite Difference stencil (FD). In space this stencil shows a standard symmetric central difference scheme (CDS) for the diffusive term and a second-order linear upwinding difference scheme (LUDS) for the convective term. CDS could also be applied for the convective term, but we found unacceptable numerical oscillations at higher reaction rates. In time Crank-Nicolson (CN) for all time steps except for the last one was applied – here the discrete form of the mirror symmetry between the two profiles at the beginning of the half period ($t = 0$) and the end ($t = \Delta t_{cyc}$) were directly formulated as

$$T(z_i, t = 0) - T(L - z_i, t = \Delta t_{cyc}) = 0. \tag{5}$$

The mass balance is assumed to be quasi-steady state due to the dominating transient behaviour of the energy balance. As a result, only space dicretisation schemes must be applied. We used the same CDS/LUDS approach described above for the energy balance.
Concluding from this, the presented CN - CDS/LUDS approach is approximately second order in space and time. The result of the global disretisation is a large – and due to the reaction terms – coupled and non-linear system of equations

$$\mathbf{R}(\mathbf{U}) = \tilde{M}\mathbf{U} + \mathbf{F}(\mathbf{U}) + \mathbf{D} = 0, \tag{6}$$

where $\tilde{M}$ includes the discrete transport operator while $\mathbf{F}(\mathbf{U})$ and $\mathbf{D}$ account for reaction and spatial boundary conditions. The solution vector $\mathbf{U}$ contains the nodal unknown values for the temperature and N_2O concentration. We found for the considered examples that about 50 grid points in time and 100 grid points in space are sufficient to obtain a grid independent solution. According to

$$neq = ns * nt * npde \tag{7}$$

the overall number of unknows is about 1000. In this formula ns and nt depict the number of grid point in space and time and $npde = 2$ represents the number of (partial) differential equations to solve.

Since the ignition-extinction diagrams exhibit turning points in which simple path continuation algorithms fail, we used Keller's arc-length-continuations technique in the same way as it is described in [19]. The nonlinear equation were solved by Newton-Raphson's method with a stopping criteria of $||\mathbf{R}(\mathbf{U})||_{\mathbf{2}} \leq \mathbf{10^{-6}}$. The arising linear equations were then efficiently solved by the use of modern direct solvers implemented in the free of charge UMFACK2.1 package [4]. The Newton-Raphson method turned out to be quite robust in our case and usually 3-5 nonlinear iterations were required to meet our stopping criteria. A complete solution branch was calculated in approximately 500 steps using an empirical step-size control described in [5].

Table 1: Physical and chemical parameters (for average mass fraction $w_{N_2O} = 0.1$, reference temperature $T = 500\ °C$).

symbol	*value*	*unit*		*symbol*	*value*	*unit*	
a_v	1100.0	$[\frac{m^2}{m^3}]$	[18]	ε	0.69	$[-]$	[6]
L	1.5	$[m]$	[6]	D	0.12	$[m]$	[6]
d_{hyd}	$2.\cdot 10^{-3}$	$[m]$	[6]	C^0	$0 - 0.1$	$[\frac{mol}{m^3}]$	
$D_{eff,g}$	$6.91 \cdot 10^{-3}$	$[\frac{m^2}{s}]$	[9, 14]	$c_{p,g}$	1093.0	$[\frac{J}{kgK}]$	[9, 23]
λ_g	0.1	$[\frac{W}{mK}]$	[9]	ϱ_g	0.486	$[\frac{kg}{m^3}]$	[9, 23]
λ_s	1.26	$[\frac{W}{mK}]$	[9]	$c_{p,s}$	840.0	$[\frac{J}{kgK}]$	[18]
λ_{eff}	0.85	$[\frac{W}{mK}]$	[9]	ϱ_s	1645.0	$[\frac{kg}{m^3}]$	[9]
k_{wv}	30.0	$[\frac{W}{m^2K}]$	[6]	T^{amb}	300.0	$[K]$	
$\Delta H_r^{N_2O}$	$-81.6 \cdot 10^3$	$[\frac{J}{mol}]$	[23]	k_0^{hom}	$4.4 \cdot 10^{11}$	$[\frac{1}{s}]$	[6]
E_A^{hom}	$2.5 \cdot 10^5$	$[\frac{J}{mol}]$	[6]	k_0^{het}	$3.0 \cdot 10^8$	$[\frac{1}{s}]$	[6]
E_A^{het}	$1.5 \cdot 10^5$	$[\frac{J}{mol}]$	[6]	R	8.3144	$[\frac{J}{molK}]$	
α	91.0	$[\frac{W}{m^2K}]$	[14]	Δt_{cyc}	$180.-1080$	$[s]$	
β	0.18	$[\frac{m}{s}]$	[14]	v_g	0.4	$[\frac{m}{s}]$	

3 Structured catalyst beds and separation of hybrid reaction

Before the concept of strutured catalyst beds is presented, it is necessary to explain why there is a need for the separation of the hybrid reation into its parts. There are two fundamental answers to this, depending on the the point of view. First of all, looking from the operational viewpoint, it makes sense to minimize or even avoid homogeneous reactions totally because homogeneous reactions lead to high temperature levels and so they might irreversibly damage the activity and/or structural stability of the monolith. The suppression of homogeneous reaction can be achieved by realizing the idea of axially aligned inert/active sections. The insertion of inert sections generally enables the operator to work with lower maximum temperatures inside the reactor. This effect is based on modification of the reaction zone which is widened in comparison to that of an unstructured catalyst. The second explanation should be stressed in the context of the presented project: By means of the structured catalyst bed the heat of reaction is broken down into parts which is shown in Fig. 3.

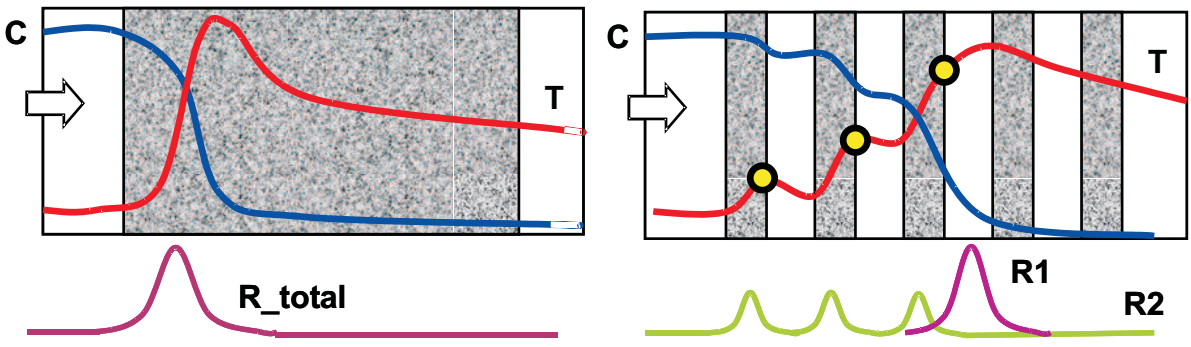

Figure 3: Scheme of reaction for a conventional catalyst (left) and for a structured catalyst (right). Course of temperature T, concentration C and reaction rates (r_{hyb},r_{hom}, r_{het}) are shown. Grey and white areas depicts active and inert section.

On the one hand decelerating the reaction broadens the reaction zone. On the other hand having discrete chemical 'discontinuities' (in which the active and the inert section are neighbored) gives us prominent points of interest inside the reactor (cf. Fig. 3). Forcing the stretched profiles to move over whole catalytic structure and in particular over the discontinouities will help to further understand the chemical and thermal coupling mechanisms.

In previous experiments and simulations of the hybrid N_2O decomposition it was found that the variation of genuine parameters (switching time, inlet concentration and flow rate) alone did not lead to the desired separation of the hydrid reaction [6].

In addition, attempting to chemically disturb the hybrid reaction e.g. by means of some dosage of iodine, did not succeed [6]. Certainly, the reason for this behavior can be found in the comparably small temperature window between the two reactions types. The heat production of the catalytic reaction nearly always leads to the ignition of the thermal reaction. We observe that as a result, most operating conditions lead to a spatially and temporally smeared hybrid reaction zone. One way of circumvending this effect would be to create complex temperature control. For example this could be realized by cooling coils which limit the heat of reaction and suppress the thermal reaction. Another much simpler way to exert influence is to apply an axially structured catalyst inside the RFR. Alternating active and inert axially aligned monolithic sections which have similar physical properties, make it possible to establish a kind of chemical 'switch'. Fig. 3 shows the basic principle of this idea.

Considering the catalytic reaction taking place in the first active section (cf. Fig. 3, right), depending on the heat amount produced **and** temperature level prevailing at the end of the section, the gas either continues reacting having passed the border to the neighbouring inert section or the reaction extinguishes. The number of possible arrangements of sections for a structured catalyst bed tend to be unlimited. Below, we list the 'geometric' parameters which during simulations have been detected as having a strong influence on the hybrid reaction:

1. Overall relation between active/inert area.
2. Number of sections.
3. Width of sections.
4. Position of sections.

In combination with reverse flow operation, the idea of a structured catalyst as a diagnostic method for hybrid reactions becomes complete since all fronts move inside the monolith. Due to the inherent time-dependency of instationary fixed bed processes, the amount of measurable data is much higher than it would be in a stationary operated conventional fixed bed reactor. Qualitative changes can now be detected in space and time (within a half-period).

4 Results and discussion

We present experimental and theoretical results for an appropriate arrangements of sections in order to separate the hybrid N_2O decomposition. It is a fact that it is easier to change the key parameters in the simulation, rather than in the experimental setup itself. It should be emphasized that the modification of the monolith catalyst is a very costly and time-consuming procedure.

4.1 Variation of geometric parameters

Due to restrictions of the existing RFR, the above described segmentation could only be applied in the center area between 45 cm and 105 cm. The remaining parts are inert and contain heating

coils needed for the start up phase. Numerous ignition-extinction diagrams were calculated for kinds of combinations of geometric parameters listed above. A proportion of 50% passive and 50% active area seemed to be appropriate for clear separtion of the hybrid reaction. Nevertheless, the cases with less overall catalytic area (40/60 and 30/70) lead to similar results. Number and position of the section on the other hand had a much stronger influence on the macroscopic behaviour. Higher number of sections tend to a better separation of the hybrid reaction but from the experimental point of view the width should not be too small. Fig. 4 shows a scheme of a structured catalyst which was eventually realized for the experiments. It can clearly be seen where the alternating catalytic zones (C) and passive inert zones (I) are located. All catalytic active sections have the same width of 7.5 cm which is roughly the size of a typical reaction zone found in earlier studies by our group [13]. The experimental setup provides 19 thermo-elements closely equidistributed along the cylinder axis. The position of these elements is denser in the center to achieve a higher resolution and to ensure that at least one element is present in each section.

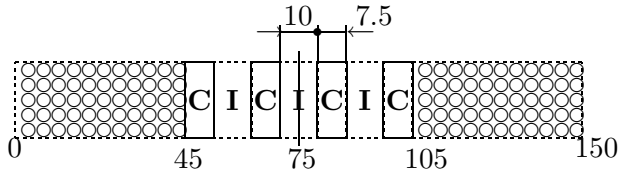

Figure 4: Scheme of the realized structured catalyst inside the RFR. Values in cm.

4.2 Variation of operating parameters

After the geometric setup of the structure was selected the variation of essential operating parameters such as switching time, N_2O concentration (or corresponding percentage by weight $w_{N_2O}[\%]$) and flow rate can easily be varied in both the simulation and the experiments. For a constant flowrate of $\dot{V} = 100\ l/min$ the experiments and simulation studies were based on the program listed in Table 2. After the percentage by weight of N_2O was selected inert nitrogen N_2 was added until the flowrate of $\dot{V} = 100\ l/min$ was reached.

Table 2: Operating parameters set for calculation and experiment.

Δt_{cyc} [s]	$w_{N_2O}[\%]$	$w_{N_2}[\%]$	$C_{N_2O}[mol/m^3]$
180	14	86	1.6
180	18	82	2.0
180	22	78	2.4
360	14	86	1.6
360	18	82	2.0
360	22	78	2.4
720	14	86	1.6
720	18	82	2.0
720	22	78	2.4
1080	14	86	1.6
1080	18	82	2.0
1080	22	78	2.4

The comparison between experiment and simulation is of crucial importance of the presented work. Experiments in general help improving the used theoretical model consisting of the bal-

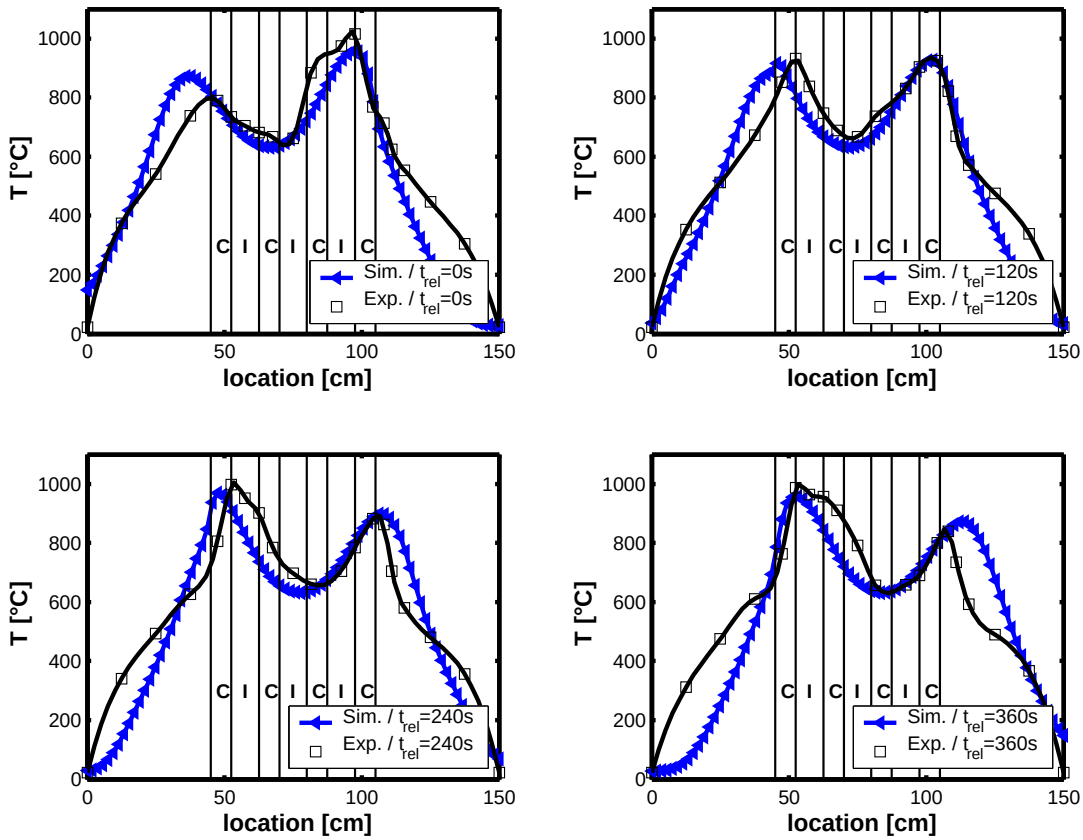

Figure 5: Satisfying temporal ($t_{rel} = 0s, 120s, 180s, 360s$) and spatial agreement between simulation and experiment. Inlet concentration $C = 2.4\ mol/m^3$ and switching time $\Delta t_{cyc} = 360s$.

ance equations and physical and kinetical parameters. Moreover, the exact behaviour of the hybrid reaction can not be understood by experimenting alone since one can nearly only measure the temperature inside the reactor. Data of the spatial distribution of concentration is very hard to collect and a direct detection of the reaction rate itself nearly impossible to achieve.
Fig. 5 verifies by means of the temperature that the calculated and experimentally retrieved data nearly matches. The four subfigures account for different times within one half cycle and help us to conclude that the temeprature profiles are qualitatively of the same shape in space and time. The calculated local extremes of the temperature predict the experimental results very well. Two obvious differences can be found. On the one hand the calculated temperature fronts are moving faster and in a wider range than the experiments show. On the other hand it is apparent that the curvature of the profiles deviates considerably in the outer heating zones. The reason for this can be explained by an use constant gas velocity and porosity in the simulated model equations.

Fig. 6 presents a compact comparison of experiment and simulation for a short switching time of $\Delta t_{cyc} = 180s$ and average inlet concentration of $C = 2.0\ mol/m^3$. In the top left diagram, one can see a ignition-extinction bifurcation based on the energy norm of the temperature against the inlet concentration. Depicted is a section of the ignited branch. The difference in curvature which is explained above leads to mutually displaced curves representing the experiment and simulation. The full temperature behaviour in space and time (over one half cycle) is represented in the top right diagramm. Underneath, two figures complete the comparison by showing the two simulated single reaction rates also in space and time.

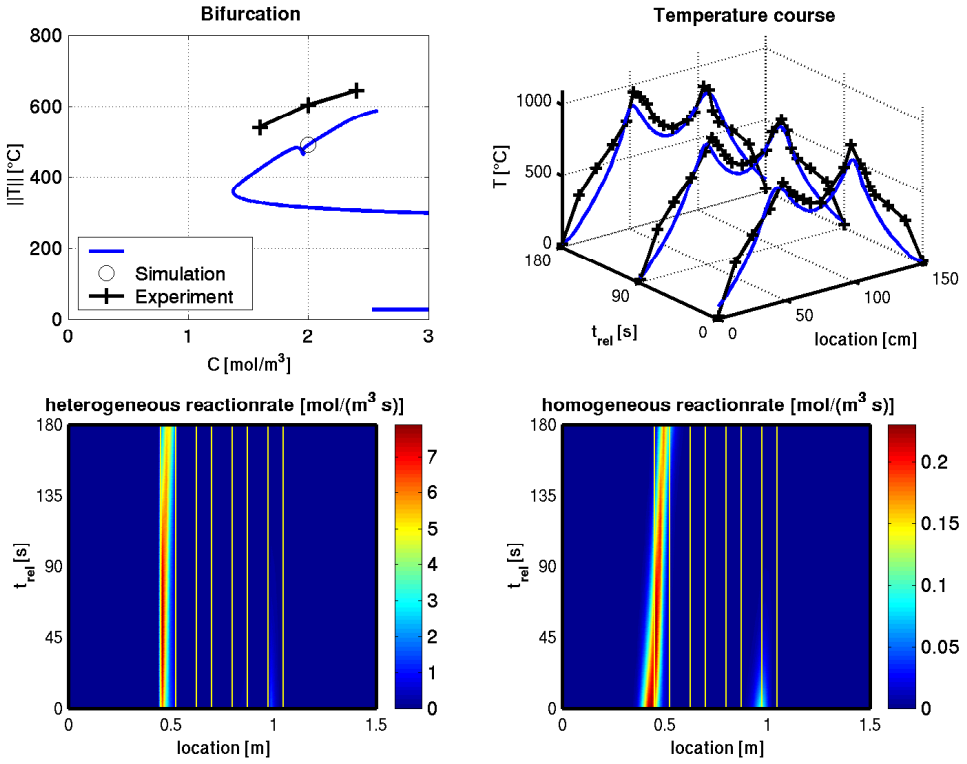

Figure 6: Comparison of experiment and simulation (switching time $\Delta t_{cyc} = 180s$, concentration $C = 2.0\ mol/m^3$).

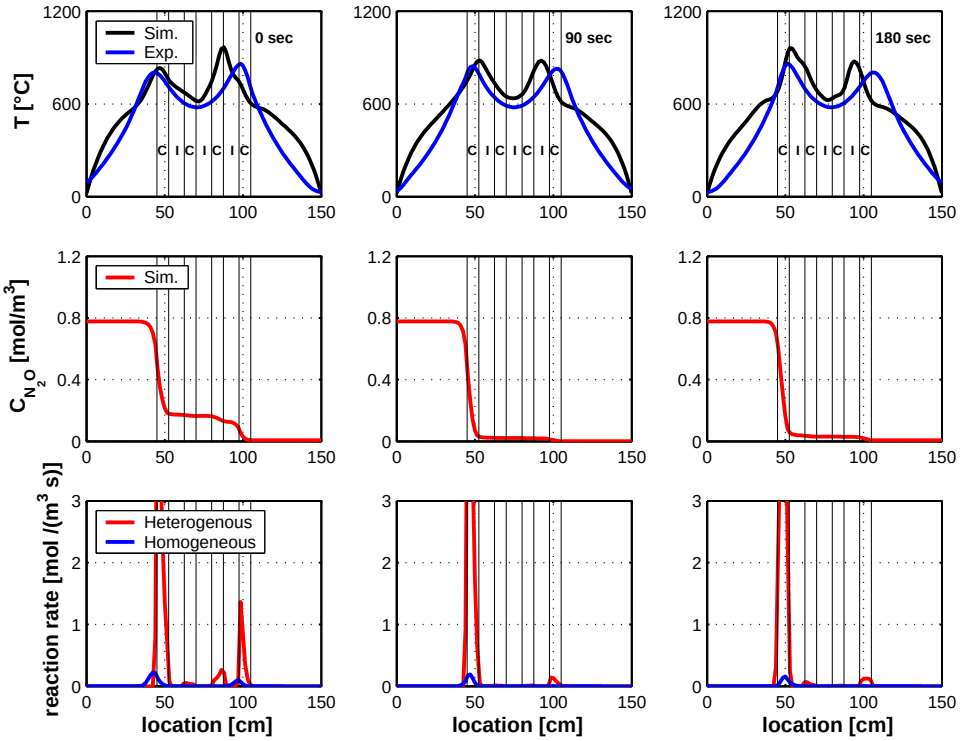

Figure 7: For lower switching times, e.g. $\Delta t_{cyc} = 180s$, the smeared reaction front can be seen throughout the cycle. Simulated and experimental retrieved Temperature distribution(upper), concentration (middle) and reaction rates (down) are depicted.

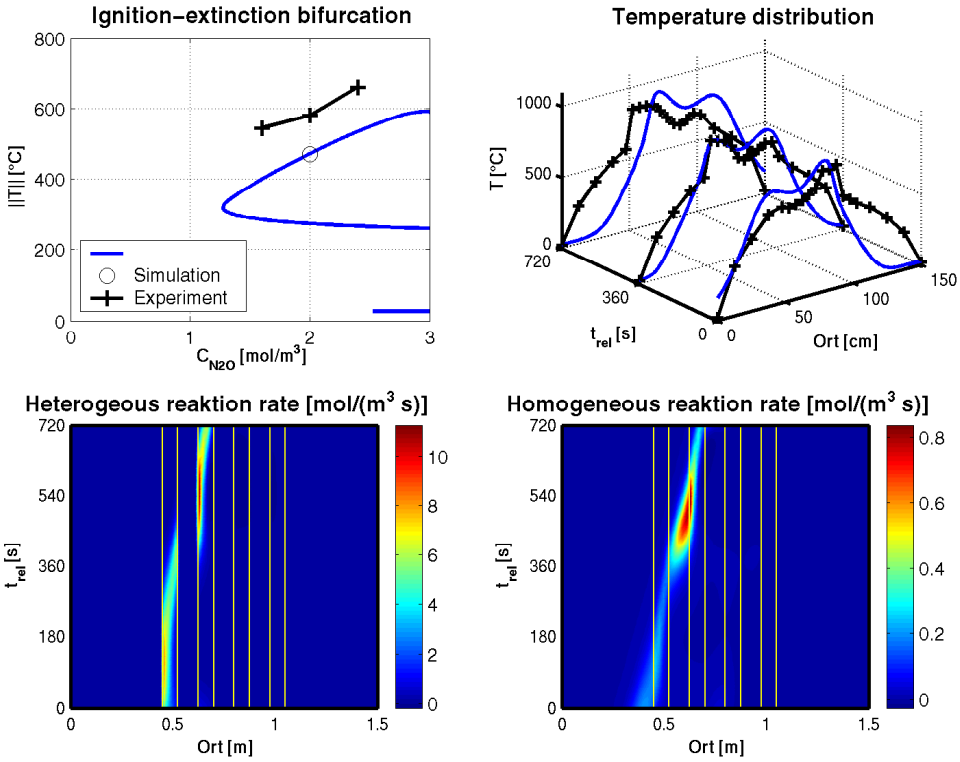

Figure 8: Comparison of experiment and simulation (switching time $\Delta t_{cyc} = 720s$, concentration $C = 2.0\ mol/m^3$).

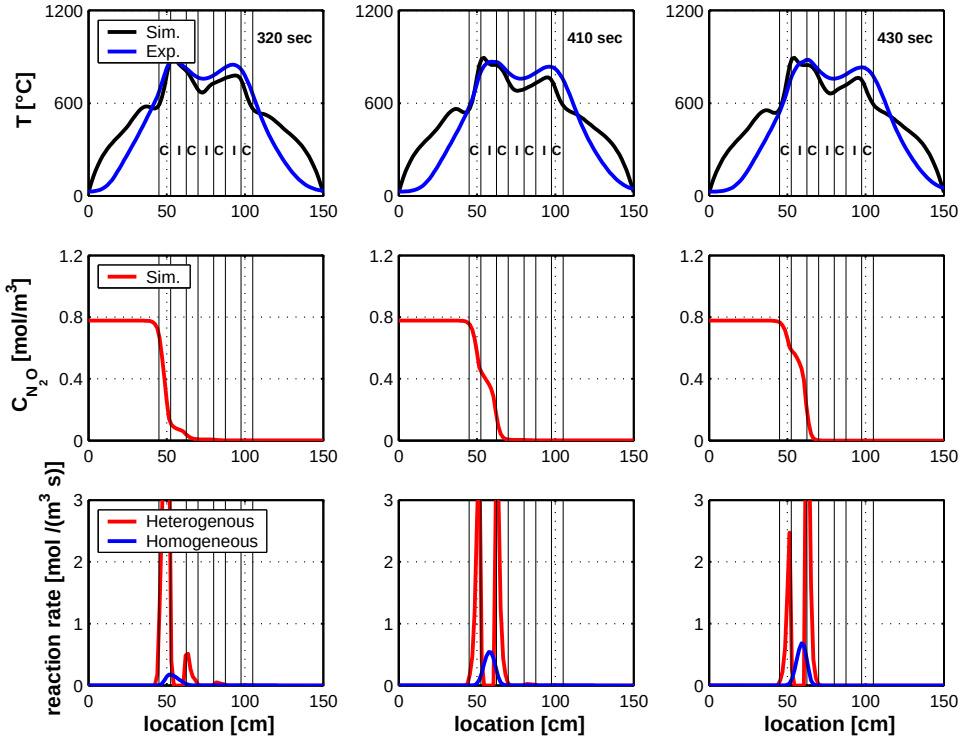

Figure 9: For higher switching times, e.g. $\Delta t_{cyc} = 720s$, the separation reaction front can clearly be seen in the middle of the cycle. Simulated and experimental retrieved Temperature distribution(upper), concentration (middle) and reaction rates (down) are depicted.

In this specific case we cannot observe the desired splitting of the reaction zone. In fact, the location of the thermal and catalytic reaction zones almost completely coincide. This phenomenon is presented in more detail by looking at Fig. 7. Here, the spatial distribution of temperature, concentration and the two reaction rates is diplayed for the beginning, middle and end of the half-cycle ($t = 0s, 90s, 180s$). As stated before the two reaction rates nearly completely coincide. As a consequence, except for the very beginning at $t = 0s$, almost the full conversion ($> 95\%$) takes place in the first catalytic section. In addition, one can conclude that for this low switching time the two inner catalytic section remain unused and as a consequnce violate our idea of breaking down the reaction into portions.

By means of the second presented case the crucial influence of the switching time becomes clear as assumed in before. Fig. 8 shows the case study for the same inlet concentration as in the first case but for a much higher switching time of $\Delta t_{cyc} = 720\ s$. This leads to a more characteristic RFR behaviour, whereas for $\Delta t_{cyc} = 180\ s$ the behaviour essentially tends to represent a counter current flow reactor (CFR).

At the beginning of the cycle the reaction is essentially of the heterogeneous-catalytic type. But with advancing time the catalytic reaction extincts and due to the high temperature level, an ignition of the homogeneous-thermal reaction can be observed. Regarding (relative) time this accour after $320s$ and regarding space directly after the first catalytic active monolith section. Fig. 9 clearifies the effect of consecutive extintion and ignition by means of three snapshots for $t = 320s, 410s$ and $430s$ (relative) time in the same way as in Fig. 7. In the first column (at $t = 320s$) the homogeneous reation has just begun. The temperature at the border of the two first monolith section offers that this happens at about $T = 850\ °C$ which is remarkebly the same ignition temperature for the homogeneous reaction as found in the literature [3]. Moreover, due to the larger switching time here, the two inner catalytic section are needed. It can clearly be seen from the spatial distribution of concentration and reaction throughout the cycle that in the first two catalytic sections and the embraced inert section reaction takes place (as a consequence after the flow reversal this would be true for the other side).

5 Summary and Conclusion

Structured catalysts in combination with reverse-flow operation have a significant influence on the way hybrid reactions take place. We have shown boths by simulation and by experiments in an technical scale RFR that the two types of reaction - heterogeneous-catalytic and homogeneous-thermal - of N_2O decompositions could be successfully split by arranging appropriate positioned inert zones inside the reactive zone in the centre of the RFR. It can be observed that for higher switching times, 720 s and more, a process with consecutive ignition and extinction of the two reaction types can take place. Remarkably the use of a structured catalyst does not lead to a significant change on the overall (macroscopic) ignition-extinction diagram.
Since the reaction itself is hardly possible to measure and even the concentration is only known at the inlet and outlet of the RFR simulation are inevitable for detailed understanding. Looking on the comparable coarse gridding of the thermo elements simulated and experimentally retrieved data are in satisfying good agreement.

Acknowledgement This work became possible by the promotion of the Deutsche Forschungsgemeinschaft (DFG). The author would like to thank Ch. Fredebeul for continuous support. A special thank belongs to Rafael Dyll.

Notation

a_v	volumetric surface
$c_{p,g}$	constant pressure heat capacity of gas
$c_{p,s}$	constant pressure heat capacity of monolith
C	catalyst section
C^0	molar inlet density
d_{hyd}	diameter of monolith channel
D	diameter of tubular reactor
$D_{eff,g}$	effective gas phase diffusion coefficien
E_A^{hom}	activation energy of homogeneous reaction
E_A^{het}	activation energy of heterogeneous reaction
$\Delta H_r^{N_2O}$	enthalpy change of decomposition
I	inert section
k_{wv}	heat loss constant
k_0^{hom}	rate constant of homogeneous reaction
k_0^{het}	rate constant of heterogeneous reaction
L	length of reactor
r	radius of reactor
r_{hom}	homogeneous reaction rate
r_{het}	heterogeneous reaction rate
r_{hyb}	hybrid reaction rate
R	universal gas constant
t	time
t_{rel}	relative time
Δt_{cyc}	switching time
T^{amb}	ambient temperature
v_g	gas velocity
$\dot{V}$	volumetric flow rate
z	space coordinate
$\mathbf{R}(\mathbf{U})$	vector of residuals
$\tilde{M}$	dicrete transport operator
$\mathbf{U}$	vector of unknowns
$\mathbf{F}(\mathbf{U})$	vector of reactive terms
$\mathbf{D}$	vector of boundary conditions

greek letters

α	heat transfer coefficient
β	mass transfer coefficient
ε	viod fraction
λ_g	heat conduction coefficient of gas
λ_s	heat conduction coefficient of gas
λ_{eff}	effective heat conduction coefficient
ϱ_g	gas density
ϱ_s	solid density
$\mathbf{\Omega_{dyn}}$	computational domain of dynamical simulation
$\mathbf{\Omega_{VD}}$	computational domain of global discretization

References

[1] Agar, D.W., Galle, M., Watzenberger, O., 2001 Thermal N_2O Decomposition in Regenerative Heat Exchanger Reactors. *Chem. Ing. Sci.*

[2] Björck, A., Dahlquist, G., 1972, Numerische Methoden, *R. Oldenbourg Verlag, München* **Auflage 1**.

[3] Bamford, C.H., Tipper, C.F.H., 1972, Chemical kinetics. *Elsevier publishing company, Amsterdam, London, New York, 2nd edition*

[4] Davis, T.A., Duff, I.S., 1997, *A Combined Unifrontal/Multifrontal Method for unsymmetric Sparse Matrices*, Technical Report TR-97-016, Computer and Information Science and Engineering Department, University of Florida

[5] Doedel, E., 1997, Lecture notes - Numerical analysis of bifurcation problems, *Summerschool Hamburg*

[6] Galle, M., 2001, Hybride homogene und heterogene Reaktionsführung in Hochtemperatursystemen am Beispiel der Lachgaszersetzung, *Ph.D.thesis, University of Dortmund*

[7] Baerns, M., Hofmann, H.,Renken, A., 1987, Chemische Reaktionstechnik - Lehrbuch der Techischen Chemie, Band **1**, **15**.

[8] Khinast, U., Gurumoorthy, A., Luss, D., 1998, Complex Dynamic Features of a Cooled Reverse-Flow Reactor. *A.I.Ch.E.J.* **44**. 1128ff

[9] Nieken, U., 1993, Abluftreinigung in katalytischen Festbettreaktoren bei periodischer Strömungsumkehr. *Ph.D.thesis, University of Stuttgart*

[10] Glöckler, B., Kolios, G., Eigenberger, G., 2003, Analysis of a novel reverse-flow reactor concept for autothermal methane steam reforming, *Chem. Eng. Sci.* **58**, 593-601

[11] Nowak, U., Frauhammer, J., Nieken, U., 1996, A Fully Adaptive Algorithm for Parabolic Partial Differential Equations in one Space Dimension, *Computers Chem. Engng.* **20**, 547-561

[12] Wolff, Ch., 1999, Konzeption und Aufbau einers Reaktors mit periodischer Strömungsumkehr zur Diskriminierung gekoppelter homogener und heterogener Reaktionsbeiträge bei der Lachgaszersetzung, *Diploma-thesis, University of Dortmund*

[13] Nalpantidis, K., 2003, Untersuchung der heterogen/homogen Zersetzung von N_2O in einem periodisch betriebenen Festbettreaktor, *Diploma-thesis, University of Dortmund*

[14] Platte, F., 2000, Untersuchungen zum nichtlinearen dynamischen Verhalten des Reverse Flow Reactors im Hinblick auf die Diskriminierung gekoppelter homogener und heterogener Reaktionsbeiträge bei der N_2O-Zersetzung, *Diploma-thesis, University of Dortmund*

[15] Platte, F., Fredebeul, C., 2000, *Dynamische und stationäre Simulation des Reaktionsverhaltens eines Strömungsumkehrreaktors*, Ergebnisberichte Angewandte Mathematik Nr. 190 - T, Uni Dortmund

[16] Platte, F., Fredebeul, C., 2001, *Zur Anwendung direkter Löser bei der direkten Berchnung periodisch stationärer Zust"ande eines Strömungsumkehrreaktors*, Ergebnisberichte Angewandte Mathematik Nr. 197 - T, Uni Dortmund

[17] Platte, F., Galle, M., Agar, D.W., Fredebeul, C., 2001, Complex dynamic behaviour of a Reverse Flow Reactor with a hybrid reaction system.

[18] Product information sheet. Company Degussa

[19] Salinger, A.G., 1996, The Direct Calculation of Periodic States of the Reverse Flow Reactor - I. Methodology and Propane Combustion Results, *Chem. Eng. Sci.* **51**, 4903-4913

[20] Salinger, A.G., 1996, The Direct Calculation of Periodic States of the Reverse Flow Reactor - II. Multiplicity and Instabiliy, *Chem. Eng. Sci.* **51**, 4915-4922

[21] Mahesh Somani, Sanjay Viswanath, Johannes Khinast and Dan Luss., 1997, Maximum temperature in a reverse-flow-reactor with two independet reactions. *Chem. Eng. Sci.* **51**, 2483-2495

[22] Seydel, R., 1990, Practical bifurcation and stability analysis - from equilibrium to chaos. *Springer Verlag, New York* **2nd Edition**

[23] VDI-Wärmeatlas, 2002, Berechnungsblätter für den Wärmeübergang 9. Auflage, VDI Verlag

[24] Wanker, R., 1999, Entwicklung eines heterogenen Modells zur Entwicklung eines monolithischen Katalysators, Technische Universität Graz

[25] Platte, F., Galle, M., Agar, D.W., Fredebeul, C., 2001, Stabilitätsanalyse zur Diskriminierung hybrider Reaktionsbeiträge am Beispiel der N_2O-Zersetzung in einem Strömungsumkehrreaktor (SUR), XXXIV. GVC-Jahrestreffen Deutscher Katalytiker - Fachtreffen Reaktionstechnik, Weimar

[26] Matros, Yu. Sh., 1989, Catalytic processes under unsteady-state conditions. *Studies of surface Science and catalysis* **43**,. Amsterdam, Elsevier

[27] Matros Yu. Sh., Boreskov, G. K., Lahmostov, V. S., Volkov, Yu. V., & Ivanov, A. A., 1984, *Method of producing sulfur trioxide.* US Patent 4,478,808.

[28] Matros, Yu. Sh., & Bunimovich, G. A.,1996, Reverse-flow operation in fixed-bed catalytic reactors. *Catalysis Review-Science and Engineering,* 38, 1-68.

[29] Unger, J., Kolios, G., Eigenberger, G., 1997, On the Efficient Simulation and Analysis of Regenerative Processes in cyclic operation, *Comp. Chem. Eng.* **21**, 167-172

[30] Davis, M.B., Pawson, M.D., Veser, G. Schmidt, L.D., 2000, Methane Oxidation Over Noble Metal Gauzes: An LIF Study. *Comb. Flame* **123**. 159ff

[31] Nieken, U., Kolios, G., Eigenberger, G., 1994, Fixed-Bed-Reactors with Periodic Flow reversal: Experimental Results for Catalytic Combustion, *Catalysis Today* **20**, 355ff